

Design of a Micro Multi-Axis Force-Moment Sensor

Non-member	Dao Viet Dzung	Ritsumeikan University
Member	Toshiyuki Toriyama	New Energy and Industrial Technology Development Organization
Non-member	John Wells	Ritsumeikan University
Member	Susumu Sugiyama	Ritsumeikan University

ABSTRACT

The design concept and theoretical investigation of a micro multi-axis force-moment sensor utilizing the piezoresistive effect in silicon are described. The purpose of the sensor development is to measure the force and moment acting on boundary particles in a turbulent liquid flow. The sensor is designed to independently detect 3 components of force and 3 components of moment in three orthogonal directions. Conventional p-type and four-terminal p-type piezoresistors have been combined in a single sensing chip in the plane (111) of silicon.

Keywords: *piezoresistive effect, micro force-moment sensor, 6 degrees of freedom, FEM analysis*

1 INTRODUCTION

Recently, the demands for micro force sensors in robotics, hydraulics, automobiles and other applications are increasing. There have been substantial research and fabrication of micro force sensors. Some examples of these are the three-component force sensors [1,2], normal force sensor [3], shear force sensor [4], and three-dimensional tactile sensors [5,6]. While much work has dealt with three-component force sensors, studies in six force-moment components micro sensors are very rare. The three-component sensors are adequate for the tasks involving feature identification, or determining object location. However, for certain applications, they are inadequate [7]. Examples of such applications include measuring external forces on particles in liquid flows, and grasping and manipulation by robot hand. There have been several approaches to design and fabricate full six-component force sensors. Sinden and Boie [8] introduced some theoretical designs of a planar capacitive force sensor with six degrees of freedom (6-DOF). However, these designs are more complex than piezoresistive sensors and not economic to fabricate with MEMS in terms of fabrication accuracy, reproducibility, and sensor dimension. Some centimeter-scale conventional 6-DOF force sensors have also been presented [9,10], in which the metallic strain gauges were fixed on spatial structure. These sensors are very complicated structurally and have low sensitivity. Grahn [7] invented a triaxial normal and shear force sensor, which used ultrasonic technique as the detecting principle. Okada [11] also reported a planar six-axis force sensor based on the silicon piezoresistive effect. Forty-eight piezoresistors are formed at twenty-four places on the upper surface of beams. This structure, then, was bonded on the surface of a strain generative body. Large numbers of piezoresistors on beams make the electrical

circuit complicated, and result in high power dissipation, wide beams, and consequently, high structural stiffness.

In this paper, a piezoresistive-based micro sensing chip with 6-DOF using only 16 conventional and 2 four-terminal piezoresistors is described. The configuration of a specific sensor to measure forces and moments acting on particles in turbulent liquid flows is also briefly presented. One can use this design of sensing chip to fabricate other micro integrated force-based devices, such as tactile sensors, and micro multi-axis accelerators.

2 THE CONFIGURATION OF SENSOR

The sensor configuration is shown in Fig. 1. The sensing chip is located inside a test particle so that its centroid coincides with the center of the surface of the sensing chip. The test particle has a diameter of about 8 mm and is made of polyethylene, of which the specific gravity is

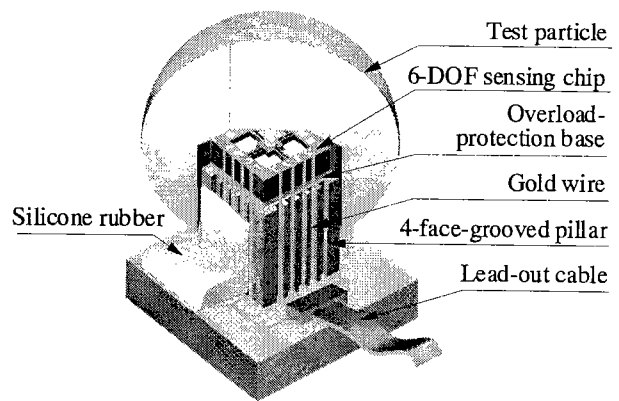


Figure 1. Configuration of the sensor.

0.965, [12], nearly equal to that of water. By this selection of material, the vertical force component (buoyancy force) on the particle is almost eliminated during working. 25 μm -diameter gold wires connecting the sensing chip to the off-chip circuits are isolated and fixed on the surfaces of a base pillar. The sensing chip is completely overload-protected by a protection base located under it. All electrical elements of the sensor are waterproofed by a silicone rubber layer. Forces and/or moments from liquid flow acting on the test particle will be transmitted to the sensing chip via a force transmission pillar placed at the center of the sensing chip. Consequently, the sensing areas will be deformed and the resistance of the piezoresistors will change, thus changing the output of the corresponding bridge circuits.

3 DESIGN OF SENSING CHIP

3.1 Dimensions of Sensing Chip

The dimensions of the sensing chip were tentatively specified based on the expected ranges of force and moment acting (horizontal forces F_x , F_y of about 1 N, and moments around X or Y axes of about 10 $\text{N}\mu\text{m}$, Fig. 2) and the desired sensitivity, the piezoresistive effect of silicon, the non-buckling condition, and the necessary width of beam for wiring. This model was then analyzed by FEM to investigate more fully the stress field in the structure, and to refine the specifications of the beam dimensions. Figure 2 shows the finite element model of the sensing chip for numerically analyzing in MENTAT 3.1 software (MARC Research Corp.). The dimensions of each arm of the crossbeam: length x width x thickness are 500 x 120 x 40 μm^3 . A total of 9156 three-dimensional solid elements (MARC element class hex 8), with 12771 nodes were used to mesh the model. The model was densely meshed in the beam to better resolve the stress distribution there. Two lateral faces of the four pedestals at the outer ends of beams are fixed as a boundary condition. For all directions in the plane (111) of Si, Young's modulus $E = 169 \text{ GPa}$ and Poisson's ratio $\nu = 0.358$, [13]. External forces and moments are applied on the central plate. Figure 3 shows the distributions of longitudinal stress components in X -axial beams due to the action of forces $F_z = 0.04 \text{ N}$, $F_x = 0.7 \text{ N}$ and moment $M_y = 12 \text{ N}\mu\text{m}$, applied consecutively. Figure 4 shows the shear stress distributions in the Y -axial beams, induced by moments $M_z = 88 \text{ N}\mu\text{m}$, $M_y = 12 \text{ N}\mu\text{m}$ and force $F_x = 0.7 \text{ N}$ also applied in turn. Stresses in the central plate are not indicated since this area is not used for sensing purposes. Piezoresistors, the properties of which will be discussed in section 3.2 below, were placed to maximize sensitivity to various components of force and moment as indicated in Figs. 3, 4 and 5. We defined the structural sensitivity S_{stL} (or structural flexibility) to an applied load L as below:

$$S_{stL} = \frac{\sigma_{max}}{L} \quad (1)$$

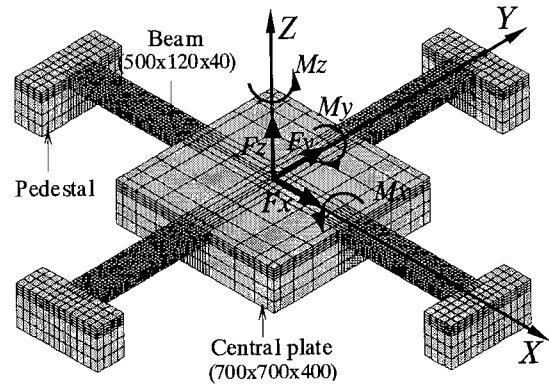


Figure 2. FEM model of sensing chip.

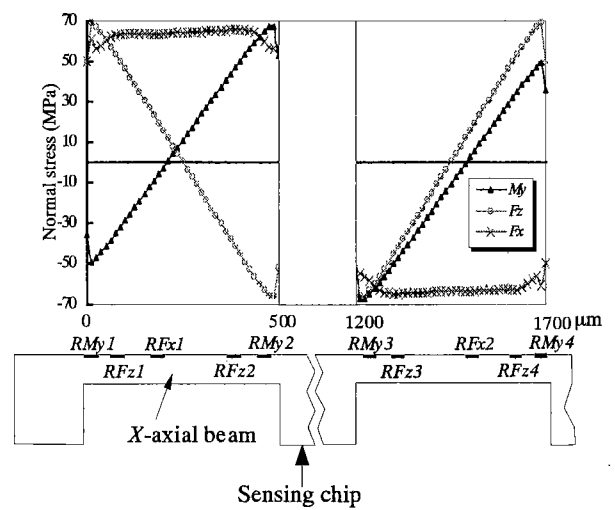


Figure 3. Normal stress distributions in X -axial beams.

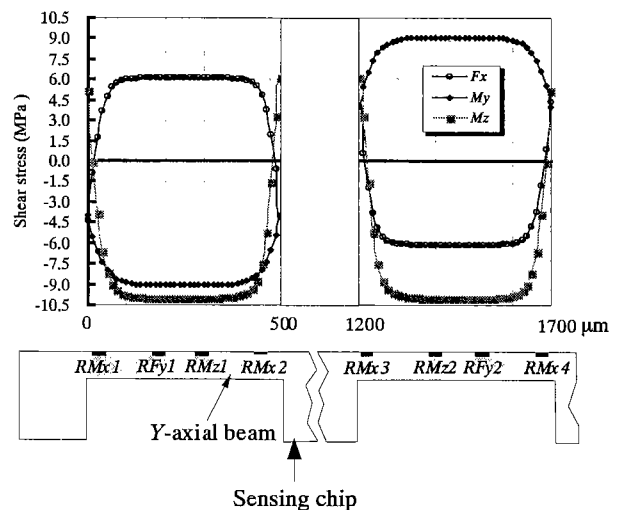


Figure 4. Shear stress distributions in Y -axial beams.

where σ_{max} is the maximum absolute stress among the stresses occurring at the various piezoresistors used in measuring that load. From Eq. (1), Fig. 3 and Fig. 4, the structural sensitivity for each component of force and moment can be obtained. In this study they are:

$$S_{stFz} = 1.25 \times 10^9 \text{ Pa/N}, S_{stFx} = S_{stFy} = 9.36 \times 10^7 \text{ Pa/N},$$

$$S_{stMx} = S_{stMy} = 5.61 \times 10^6 \text{ Pa/N}\mu\text{m}, S_{stMz} = 1.42 \times 10^5 \text{ Pa/N}\mu\text{m}.$$

The different structural sensitivities were designed to match the much larger horizontal force in liquid flow, i.e., the structural stiffness with force in the horizontal direction should be higher than that in the vertical direction to satisfy the non-buckling condition. Structural sensitivities can be balanced by changing the thickness and/or length of the beams.

3.2 Piezoresistors Arrangement

Based on the stress distribution in the crossbeam derived from FEM analysis, piezoresistors were placed and connected so as to maximize the sensitivities to various components of force and moment, and to eliminate the cross-axis sensitivities as shown in Figs. 4. Sixteen p-type conventional piezoresistors, (4- R_{Fz} , 2- R_{Fx} , 2- R_{Fy} , 4- R_{Mx} , and 4- R_{My} to detect Fz , Fx , Fy , Mx , and My , respectively), and two p-type shear piezoresistors (R_{Mz1} and R_{Mz2} to measure the moment Mz), were formed by using impurity diffusion along the central-longitudinal axes on the upper surface of an n-type silicon crossbeam, (Fig. 4). The in-plane principal axes of the piezoresistors were aligned with the crystal directions $\langle 1\bar{1}0 \rangle$ and $\langle 11\bar{2} \rangle$ of silicon (111). All conventional piezoresistors were designed to be identical, as were the two shear piezoresistors. The piezoresistive effect of conventional single-crystalline piezoresistors can be expressed as below, [14]:

$$\frac{\Delta R}{R} = \pi_l \sigma_l + \pi_t \sigma_t \quad (2)$$

where $\frac{\Delta R}{R}$ is the relative change of resistance in a conventional piezoresistor due to the longitudinal stress σ_l (i.e. the component parallel to the current flow and electrical field) and transverse stress σ_t . π_l and π_t are the corresponding piezoresistance coefficients. Piezoresistors were arranged far enough from the fixed beam-ends to avoid unexpected stress components, so that the stress status at each conventional piezoresistor is uniaxial, and as a result, $\sigma_t \approx 0$.

The piezoresistive effect of a four-terminal piezoresistor can be expressed as below, [15]:

$$V_{out} = \pi_s \tau_s V_{in} \quad (3)$$

where V_{out} is the output voltage of the four-terminal piezoresistor in response to an in-plane shear stress τ_s (or τ_{xy}), V_{in} is the supply voltage, and π_s is the shear piezoresistance coefficient. Ignoring extremely small dimensional changes of the piezoresistors, π_l and π_t are

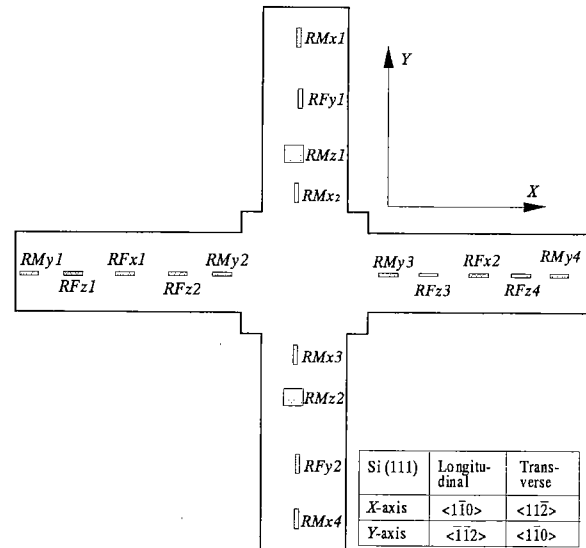


Figure 5. Arrangement of piezoresistors.

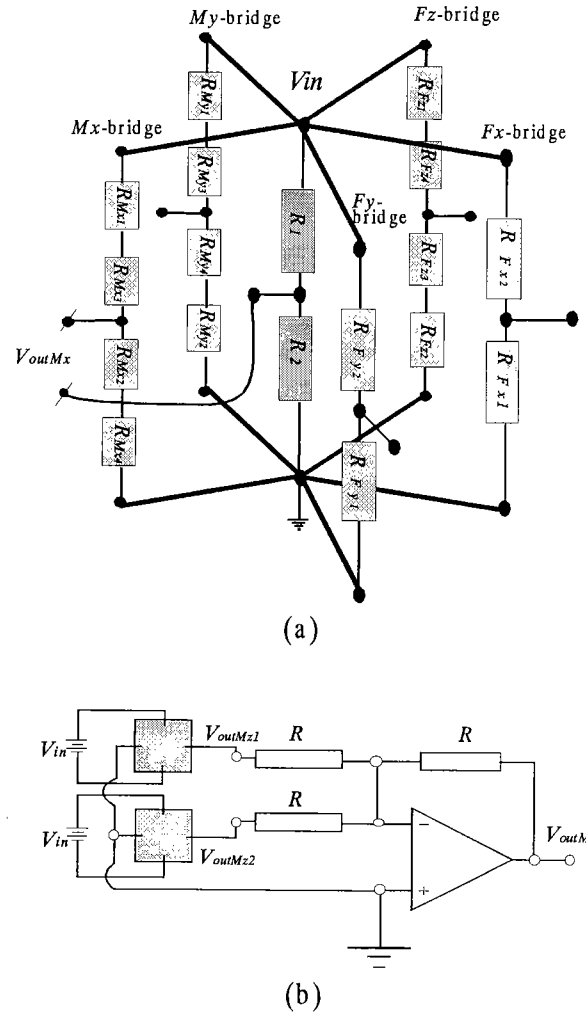


Figure 6. Measuring circuits.

constant and their values in the two crystal directions $\langle 1\bar{1}0 \rangle$ and $\langle 11\bar{2} \rangle$ can be expressed respectively by Eqs. (4) and (5) below, [16]:

$$\pi_{i\langle 1\bar{1}0 \rangle} = \pi_{i\langle 11\bar{2} \rangle} = \frac{1}{2}(\pi_{i11} + \pi_{i12} + \pi_{i44}) \quad (4)$$

$$\pi_{s\langle 1\bar{1}0 \rangle} = \pi_{s\langle 11\bar{2} \rangle} = \frac{1}{3}(\pi_{s11} - \pi_{s12} + 2\pi_{s44}) \quad (5)$$

For a bulk p-type piezoresistor with a resistivity of 7.8 Ωcm , these coefficients are $\pi_{i11}=6.6 \times 10^{-11} \text{Pa}^{-1}$, $\pi_{i12}=-1.1 \times 10^{-11} \text{Pa}^{-1}$ and $\pi_{i44}=138.1 \times 10^{-11} \text{Pa}^{-1}$, [17]. In fact, the piezoresistive coefficient of the diffused layer depends on impurity concentration and is much smaller than these bulk values, [18]. With an impurity concentration of about $5 \times 10^{19} \text{cm}^{-3}$ (typical of our process), $\pi_{i44} = 85 \times 10^{-11} \text{Pa}^{-1}$, [18]. For p-type piezoresistors, π_{i11} and π_{i12} are sufficiently small in comparison with π_{i44} , that they can be neglected. Equation (4) and Eq. (5) are thus approximated by:

$$\pi_{i\langle 1\bar{1}0 \rangle} \approx \frac{1}{2}\pi_{i44}; \quad \pi_{s\langle 1\bar{1}0 \rangle} \approx \frac{2}{3}\pi_{s44} \quad (6)$$

Substituting the coefficients in (6) into Eq. (2) and Eq. (3) with the notice explained above that $\sigma_i \approx 0$, we have:

$$\frac{\Delta R}{R} = \frac{1}{2}\pi_{44}\sigma_i = S_{gn}\sigma_i \quad (7)$$

$$V_{out} = \frac{2}{3}\pi_{44}\tau_s V_{in} = S_{gs}\tau_s V_{in} \quad (8)$$

$$S_{gn} = \frac{1}{2}\pi_{44} \text{ and } S_{gs} = \frac{2}{3}\pi_{44} \quad (9)$$

where S_{gn} and S_{gs} are the stress sensitivities of the normal and shear piezoresistors, respectively.

3.3 Electrical Circuits and Working Principle

The general measurement circuit for measuring the 5 components, (F_x , F_y , F_z , M_x , and M_y), is created by connecting in parallel 5 independent detecting potentiometer circuits together and with a common potentiometer circuit to form Wheatstone bridges sharing a common half bridge, (see Fig. 6 (a)). The resistances of the two resistors of the common potentiometer circuit (R_1 , R_2) are identical and constant. The output voltage of each bridge can be measured between the output point of each sensing potentiometer and the output point of the common one (Wheatstone bridge rule) to find the corresponding applied load. Figure 6 (a) shows one example for measuring output voltage of the M_x -bridge V_{outMx} . The output voltage of each bridge can be written as below, [19]:

$$V_{outFz} = \frac{1}{4} \left(\frac{\Delta R_{Fz1} + \Delta R_{Fz4}}{R_{Fz1} + R_{Fz4}} - \frac{\Delta R_{Fz2} + \Delta R_{Fz3}}{R_{Fz2} + R_{Fz3}} \right) V_{in} \quad (10)$$

$$V_{outMx} = \frac{1}{4} \left(\frac{\Delta R_{Mx1} + \Delta R_{Mx3}}{R_{Mx1} + R_{Mx3}} - \frac{\Delta R_{Mx2} + \Delta R_{Mx4}}{R_{Mx2} + R_{Mx4}} \right) V_{in} \quad (11)$$

$$V_{outMy} = \frac{1}{4} \left(\frac{\Delta R_{My1} + \Delta R_{My3}}{R_{My1} + R_{My3}} - \frac{\Delta R_{My2} + \Delta R_{My4}}{R_{My2} + R_{My4}} \right) V_{in} \quad (12)$$

$$V_{outFx} = \frac{1}{4} \left(\frac{\Delta R_{Fx1}}{R_{Fx1}} - \frac{\Delta R_{Fx2}}{R_{Fx2}} \right) V_{in} \quad (13)$$

$$V_{outFy} = \frac{1}{4} \left(\frac{\Delta R_{Fy1}}{R_{Fy1}} - \frac{\Delta R_{Fy2}}{R_{Fy2}} \right) V_{in} \quad (14)$$

where V_{in} is the input voltage. Note that all conventional piezoresistors mentioned here are identical.

Two four-terminal piezoresistors for measuring the moment around the Z -axis are connected together via a standard operational amplifier to form a summing circuit, [19], which performs the algebraic additional operation between the voltages V_{outMz1} and V_{outMz2} of the two piezoresistors R_{Mz1} and R_{Mz2} , respectively, (see Fig. 6 (b)).

$$V_{outMz} = V_{outMz1} + V_{outMz2} \quad (15)$$

where V_{outMz1} and V_{outMz2} are calculated from Eq. (8).

3.3.1 Detection of tangential forces F_x and F_y

- When a tangential force F_x in X -direction is applied to the sensing chip, the beam with piezoresistor R_{Fx1} will be subjected to a tensile stress, (Fig. 3), while the opposite beam, on which piezoresistor R_{Fx2} is located, will undergo a corresponding compression, hence $R_{Fx1} = -R_{Fx2}$. As a result, the output voltage of the F_x -bridge is different from zero, (see Eq. (13)):

$$V_{outFx} = \frac{\Delta R_{Fx1}}{2R_{Fx1}} V_{in}, \text{ and } S_{CFx} = \frac{V_{outFx}}{\Delta R_{Fx1}} = \frac{V_{in}}{2R_{Fx1}} \quad (16)$$

where S_{CFx} is defined as the circuit sensitivity of the F_x -bridge. By contrast, R_{Fy1} and R_{Fy2} in the Y -axial beam have no change in resistance because the normal stresses in them are mostly equal to zero. Therefore, the F_y -bridge is still balanced, *i.e.*, there is no response in this bridge, (see Eq. (14)). Similarly, the M_x -bridge has no response. In the case of the F_z -bridge, as the stresses at R_{Fz1} and R_{Fz4} have the same absolute magnitude, but in opposite sign, (Fig. 3), so $R_{Fz1} = -R_{Fz4}$. Analogously, $R_{Fz2} = -R_{Fz3}$. Therefore $V_{outFz} = 0$, so the F_z -bridge has no sensitivity to the force F_x . Similarly, the M_y -bridge has no response. In the Y -axial beam, shearing stresses with the same magnitude but opposite in sign will exist in four-terminal piezoresistors R_{Mz1} and R_{Mz2} , (Fig. 4), so the total output voltage of the Mz -circuit is still zero, (see Eq. (15)). Note that four-terminal piezoresistors with crystal directions mentioned above are not sensitive to normal stresses, (see Eq. (8)).

- The detection of tangential force F_y is analogous to F_x .

3.3.2 Detection of vertical force F_z

When a vertical force F_z is applied to the sensing chip, from the FEM result, (Fig. 3), the normal stresses in the

four piezoresistors of the Fz -bridge can be written as below:

$$\sigma_{R_{n1}} = \sigma_{R_{n2}} = -\sigma_{R_{n3}} = -\sigma_{R_{n4}}$$

where $\sigma_{R_{ni}}$ is the normal stress at piezoresistor R_{Fzi} , $i=1,4$.

Therefore, $\Delta R_{Fz1} = \Delta R_{Fz4} = -\Delta R_{Fz2} = -\Delta R_{Fz3}$. Consequently, the Fz -bridge is unbalanced, and the output response is different from zero, (Eq. (10)):

$$V_{outFz} = \frac{1}{2} \frac{\Delta R_{Fz1}}{R_{Fz1}} V_{in} \text{ and } S_{CFz} = \frac{V_{outFz}}{\Delta R_{Fz1}} = \frac{V_{in}}{2 R_{Fz1}} \quad (17)$$

where S_{CFz} is defined as the circuit sensitivity of the Fz -bridge. Due to the symmetry of the arrangement of piezoresistors and the structure of the sensing chip, the normal stresses at R_{Fx1} and R_{Fx2} are equal, (Fig. 3), hence their resistance changes are equal: $\Delta R_{Fx1} = \Delta R_{Fx2}$, so the output voltage of the Fx -bridge is equal to zero, (see Eq. (13)). Similarly, no response will occur in the Fy -bridge. Likewise, in the case of the Mx -bridge, the total resistance change of the upper arm ($\Delta R_{My1} + \Delta R_{My3}$) is equal to that of the lower arm ($\Delta R_{My2} + \Delta R_{My4}$), so the Mx -bridge is still balanced. Analogously, the response of the Mx -bridge is zero. The in-plane shear stress component is equal to zero at R_{Mz1} and R_{Mz2} , so the output of the Mz -circuit is equal to zero.

3.3.3 Detection of moment Mx and My

- When a moment My around the Y -axis is applied to the sensing chip, as can be seen from the FEM result, (Fig. 3), the normal stresses in the four piezoresistors of the My -bridge can be written as $\sigma_{R_{n1}} = -\sigma_{R_{n4}} = -\alpha \sigma_{R_{n3}} = \alpha \sigma_{R_{n2}}$, where α is a constant depending upon the width and length of the beam; in this study, $\alpha \approx 0.75$. Therefore, the resistance change in the My -bridge can be written by $\Delta R_{My1} = -\Delta R_{My4} = -\alpha \Delta R_{My2} = \alpha \Delta R_{My3}$. Substituting this relation into Eq. (12), the output voltage and circuit sensitivity of the My -bridge are expressed by:

$$V_{outMy} = \frac{1}{4} \frac{(1+\alpha)\Delta R_{My3}}{R_{My3}} V_{in} \text{ and } S_{CMy} = \frac{(1+\alpha)V_{in}}{4} \quad (18)$$

However, for the piezoresistors of the Fz -bridge, $\Delta R_{Fz1} = -\Delta R_{Fz4}$ and $\Delta R_{Fz2} = -\Delta R_{Fz3}$. Therefore, the output voltage of the Fz -bridge is zero, (see Eq. (10)). R_{Fx1} and R_{Fx2} are intentionally located at the positions where the normal stress, induced by the concentrated moment My , is equal to zero, (see Fig. 3). As a result, the Fx -bridge has no response either. The FEM analysis result has shown that these positions are unchanged when the beam thickness and/or the moment My are changed. In the Y -axial beam, the longitudinal stress is equal to zero at the piezoresistors, so the Fy -bridge and Mx -bridge have no response. Shearing stresses of identical magnitude but opposite sign exist in the four-terminal piezoresistors R_{Mz1} and R_{Mz2} , (Fig. 4), so the total output voltage of the Mz -circuit is still zero, (see Eq. (15)).

- The detection of moment Mx is analogous to My .

3.3.4 Detection of moment Mz

When a moment around the Z -axis Mz is applied to the sensing chip, only shearing stresses exist in the piezoresistors. These stresses are equal in magnitude and sign at R_{Mz1} and R_{Mz2} (Fig. 4), so the total output voltage in the Mz -circuit is non zero:

$$V_{outMz} = 2V_{outMz1} = 2S_{gs} \tau_s V_{in} = S_{CMz} S_{gs} \tau_s \quad (19)$$

where $S_{CMz} = 2V_{in}$ is the circuit sensitivity of the Mz -bridge. The other bridges have no response to these shearing stresses.

Table 1 summarizes increases and decreases of resistance of the normal piezoresistors and output voltages of the four-terminal piezoresistors due to the applied loads. The '+' and '-' signs indicate respectively an increase and decrease, '0' means unchanged and '=' means a similar change in both sign and magnitude in piezoresistors of a corresponding bridge. Shaded regions indicate where the response of the corresponding bridge is non zero.

Table 1. Resistance changes of normal piezoresistors and output voltages of shear piezoresistors.

	Fx-bridge		Fy-bridge		Fz-bridge				My-bridge				Mx-bridge				Mz-circuit	
	R_{Fx1}	R_{Fx2}	R_{Fy1}	R_{Fy2}	R_{Fz1}	R_{Fz2}	R_{Fz3}	R_{Fz4}	R_{My1}	R_{My2}	R_{My3}	R_{My4}	R_{Mx1}	R_{Mx2}	R_{Mx3}	R_{Mx4}	R_{Mz1}	R_{Mz2}
Fx	+	-	0	0	+	+	-	-	+	+	-	-	0	0	0	0	+	-
Fy	0	0	+	-	0	0	0	0	0	0	0	0	+	+	-	-	0	0
Fz	=	=	=	=	+	-	-	+	+	-	-	+	+	-	-	+	0	0
My	0	0	0	0	+	-	+	-	+	-	+	-	0	0	0	0	+	-
Mx	0	0	0	0	0	0	0	0	0	0	0	0	+	-	+	-	0	0
Mz	0	0	0	0	0	0	0	0	0	0	0	0	0	0	0	0	=	=

3.4 The General Sensitivity of Sensing Chip

From the above analysis, in response to the i^{th} component, L^i , of force or moment, the output voltage V_{out}^i is given by:

$$V_{out}^i = S^i L^i = S_g^i S_{st}^i S_c^i L^i \quad (20)$$

where S_g^i , S_{st}^i , S_c^i are the stress, structural and circuit sensitivities for that component. S_g^i is determined by Eq. (9), S_{st}^i was defined in Eq. (1), and S_c^i can be calculated following one of the equations from Eq. (16) to Eq. (19), depending on the specific component L^i . Based on Eq. (20), table 2 shows the output voltage V_{out} (mV) and stress at piezoresistors due to applied loads. The input voltage V_{in} is 5V.

Table2. Characteristics of sensing chip.

Loads		Stress (MPa)	V_{out} (mV)
Fz (N)	0.076	94.1	100
Fx or Fy (N)	1.01	94.1	100
Mx or My (N μ m)	19.39	109	100
Mz (N μ m)	124.24	17.6	100

In this paper, the sensing chip has been designed for application in hydraulics, where the horizontal force of liquid flow is much larger than that in the vertical direction, so the structural stiffness with force in horizontal direction was higher than that in the vertical direction. These sensitivities can be balanced by changing the length and thickness of the beams. The designed-sensitivity is high enough to measure the force and moment components expected to act on particles in a liquid flow.

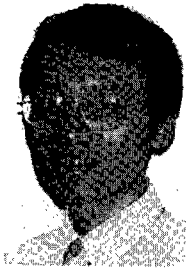
4 CONCLUSIONS

The design concept and working principle of a 6-DOF force-moment sensing chip have been presented. By combining normal and shear piezoresistors in Si (111), and the way of arranging and connecting appropriately on the sensing chip, their number was considerably reduced in comparison with prior art 6-DOF piezoresistive force sensors known to the authors; consequently, the sensing chip is smaller, more sensitive, and consumes less power. The cross-sensitivities were also completely eliminated. The sensitivity has been thoroughly analyzed, and the relation between output voltage and applied load has been established as well. This design of the sensing chip can be used to fabricate micro accelerometers, tactile sensor, and so on.

(Manuscript received June 6, 2001)

REFERENCES

- [1] Lin Wang, David J. Beebe, "A silicon-based shear force sensor: development and characterization", *Sensors and Actuators A* 84, pp33-44, 2000.
- [2] W.L. C.D. Mote, "Development and calibration of a sub-millimeter three-component force sensor", *Sensors and Actuators A* 65, pp88-94, 1998.
- [3] D. J. Beebe, A.S. Hsieh, R.G. Radwin, "A silicon force sensor for robotics and medicine", *Sensors and Actuators A* 50, pp55-65, 1995.
- [4] F. Jiang, Y. Tai, et al, "A flexible MEMS technology and its first application to shear stress sensor skin", *Proc. IEEE MEMS'97*, 1997. [5] C.T. Yao, et al, "A novel three-dimensional microstructure fabrication technique for a triaxial tactile sensor array", presented at *Proc. IEEE Micro Robots and Teleoperators Workshop*, 1987.
- [6] T. Mei, et al, "An integrated MEMS three-dimensional tactile sensor with large force range", *Sensors and Actuators A* 80, pp155-162, 2000.
- [7] Grahm, Allen R., "Triaxial normal and shear force sensor", US Patents No. RE37065, 2001.
- [8] F.W. Sinden, R. A. Boie. "A planar capacitive force sensor with six degrees of freedom", *IEEE Robot Conference Proc.*, pp.1806-1814, 1986.
- [9] Ogata, et al, "Measuring Technology", No.11, Vol.15, Japan, 1987.
- [10] C.G. Kang, "Closed-form force sensing of a 6-axis force transducer based on the Stewart platform", *Sensors and Actuators A* 2876, pp1-7, 2001.
- [11] K. Okada, "Flat-type six-axial force-sensor", *Technical Digest of The 9th Sensor Symposium*, pp.245-248, 1990.
- [12] S.B. George et al, *Materials Handbook*, ed. 4th, pp. 695, McGraw-Hill, 1997.
- [13] J.J. Wortman et al, "Young's modulus, shear modulus and Poisson's ratio in Si and Ge", *Journal of Applied Physics*, vol36, No1, pp153-156, 1965.
- [14] S.M. Sze, "Semiconductor Sensors", pp.160-185, John Wiley & Sons Inc., 1994.
- [15] Y. Kanda, "Graphical representation of the piezoresistance coefficients in Si shear coefficients in plane", *Japanese Journal of Applied Physics*, vol. 26, No. 7, pp.1031-1033, July 1987.
- [16] W.G. Pfann and R.N. Thurston, "Semiconducting stress transducers utilizing the transverse and shear piezoresistance effects", *Journal of Applied Physics*, Vol.32, No.10, pp.2008-2019, Oct. 1961.
- [17] C.S. Smith, "Piezoresistance effect in germanium and silicon", *Physical Rev.* 94, 42-9, 1954.
- [18] O.N. Tuftte, E.L. Stelzer, "Piezoresistive properties of silicon diffused layers", *Journal of Applied Physics*, vol.34, No.2, pp.313-318, 1962.
- [19] James W.D., William F.Riley, Kenneth G.Mc, *Instrumentation For Engineering Measurements*, chapter 4& 6, John Wiley & Sons, Inc. 1984.

Dao Viet Dzung (Non-member)

Dao Viet Dzung received a B.S. ('95) and M.S. ('97) in Mechanics-Informatics from Hanoi University of Technology (HUT). Currently, he is a Ph.D. student in the Graduate School of Science and Engineering, Ritsumeikan University, Japan. He worked as assistant lecturer ('95-97)

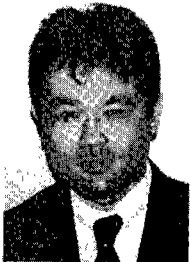
and lecturer (from '97 to the present) in Fundamentals of Machine Design Department, Faculty of Mechanical Engineering, HUT. From 1995 to 1999 he worked for Alcatel Telecom Corp. in Hanoi. His present research interests are MEMS technology and MEMS-based mechanical sensors.

includes experimental work on the structure of vortices in the turbulent boundary layer, as well as theoretical work on mechanics of interparticle contacts, and on the fluid force on a body in the presence of a vortex. He is a member of JSME and JSCE.

Susumu Sugiyama (Member)

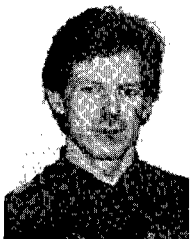
S. Sugiyama received the B.S. degree in Electrical Engineering from Meijo University, Nagoya, in 1970, and the Dr. Eng. degree from Tokyo Institute of Technology, Japan, in 1994. From 1965 to 1995, he was with Toyota Central Research & Development Laboratories, Inc.,

where he worked on semiconductor strain gages, silicon pressure sensors, integrated sensors and micromachining. While there, he was a Senior Researcher, Manager of the Silicon Devices Laboratory, and Manager of the Device Development Laboratory. Since 1995 he has been with Ritsumeikan University, Shiga, Japan, where he serves as a Professor in the Department of Robotics, Faculty of Science and Engineering. He is Vice Director of the Synchrotron Radiation Center at Ritsumeikan University, and Editor-in-Chief of *Sensors and Materials*. His current interests are microsensors and microactuators and high aspect ratio microstructure technology. He is a member of the IEEE, Japan Society of Applied Physics and the Robotics Society of Japan.

Toshiyuki Toriyama (Member)

T. Toriyama received the B.S. degree in 1985, the M.S. degree in 1987, in Mechanical Engineering from Ritsumeikan University, Shiga, Japan, and a Ph.D. degree in 1994 from Kyushu University, Fukuoka, Japan. He is now a research fellow in New Energy and Industrial Technology

Development Organization (NEDO). His current interests are piezoresistance in advanced semiconductor materials and its application to micro mechanical sensors.

John C. Wells (Non-member)

John C. Wells received a B.S. ('83) and M.S. ('87) in Agricultural Engineering from Cornell University, and a Doctorate ('92) in Mechanics from the University of Grenoble I, France. After two postdoctoral fellowships at Osaka University and Tokyo Institute of Technology, and a

year at Sharp Corporation's Print Products Development Laboratories, he has been on the faculty of Ritsumeikan University, Japan, since 1997. His research has focused on detailed mechanisms of soil erosion and particle transport by fluid flow. It